# Structure and magnetism of $La_xSr_{2-x}Co_{0.5}Ir_{0.5}O_{4-y}H_y$ (0 < x < 1) iridium-containing oxyhydride phases

James I. Murrell, Romain Wernert, Hank C. H. Wu, Benjamin M. Huddart, Stephen J. Blundell, Ronald I. Smith, and Michael A. Hayward *

## Supporting Information

## Table of Contents

**Table S7.** Parameters from the structural refinement of $La_{0.25}Sr_{1.75}CoIrO_{2.75}H_{1.25}$ against NPD data collected at room temperature.
**Figure S13.** Observed, calculated and difference plots from the structural refinement of $La_{0.5}Sr_{1.5}CoIrO_{2.5}H_{1.5}$ against NPD data collected at room temperature from the 3 different detector banks of the POLARIS instrument.
**Table S8.** Parameters from the structural refinement of $La_{0.5}Sr_{1.5}CoIrO_{2.5}H_{1.5}$ against NPD data collected at room temperature.
**Figure S14.** Observed, calculated and difference plots from the structural refinement of $La_{0.75}Sr_{1.25}CoIrO_{2.75}H_{1.25}$ against NPD data collected at room temperature from the 3 different detector banks of the POLARIS instrument.
**Table S9.** Parameters from the 2-phase structural refinement of $La_{0.75}Sr_{1.25}CoIrO_{2.75}H_{1.25}$ and $La_{0.75}Sr_{1.25}CoIrO_{3.4}H_{0.6}$ against NPD data collected at room temperature.
**Figure S15.** Observed, calculated and difference plots from the structural refinement of $LaSrCo_{0.5}Ir_{0.5}O_3H$ against NPD data collected at room temperature from the 3 different detector banks of the POLARIS instrument.
**Table S10.** Parameters from the 2-phase structural refinement of $LaSrCo_{0.5}Ir_{0.5}O_3H$ and $LaSrCo_{0.5}Ir_{0.5}O_{3.5}H_{0.5}$ against NPD data collected at room temperature.

## 4. Magnetic characterization of $La_xSr_{2-x}Co_{0.5}Ir_{0.5}O_{4-y}H_y$ phases.

**Figure S16.** Magnetization-field data collected from $Sr_2Co_{0.5}Ir_{0.5}O_{3.25}H_{0.75}$ at 300 K and at 5 K after cooling from 300 K in an applied field of 5 T.
**Figure S17.** Magnetization-field data collected from $La_{0.25}Sr_{1.75}CoIrO_{2.75}H_{1.25}$ at 300 K and at 5 K after cooling from 300 K in an applied field of 5 T.
**Figure S18.** Magnetization-field data collected from $La_{0.5}Sr_{1.5}CoIrO_{2.5}H_{1.5}$ at 300 K and at 5 K after cooling from 300 K in an applied field of 5 T.
**Figure S19.** Magnetization-field data collected from $La_{0.75}Sr_{1.25}CoIrO_{2.75}H_{1.25}$ at 300 K and at 5 K after cooling from 300 K in an applied field of 5 T.
**Figure S20.** Magnetization-field data collected from $LaSrCo_{0.5}Ir_{0.5}O_3H$ at 300 K and at 5 K after cooling from 300 K in an applied field of 5 T.
**Figure S21.** Saturated ferromagnetic moment obtained from 'ferrosubtraction' magnetization measurements plotted as a function of temperature for $La_xSr_{2-x}Co_{0.5}Ir_{0.5}O_{4-y}H_y$ phases.

## 5. Magnetic measurements in the presence of elemental Co impurities via the 'ferrosubtraction' method.

**Figure S22**. Magnetisation of $Sr_2Co_{0.5}Ir_{0.5}O_{3.25}H_{0.75}$ measured as a function of applied field at 300 K.

## 1. Structural characterization of $La_xSr_{2-x}Co_{0.5}Ir_{0.5}O_4$ ($x$ = 0, 0.25, 0.5, 0.75, 1)

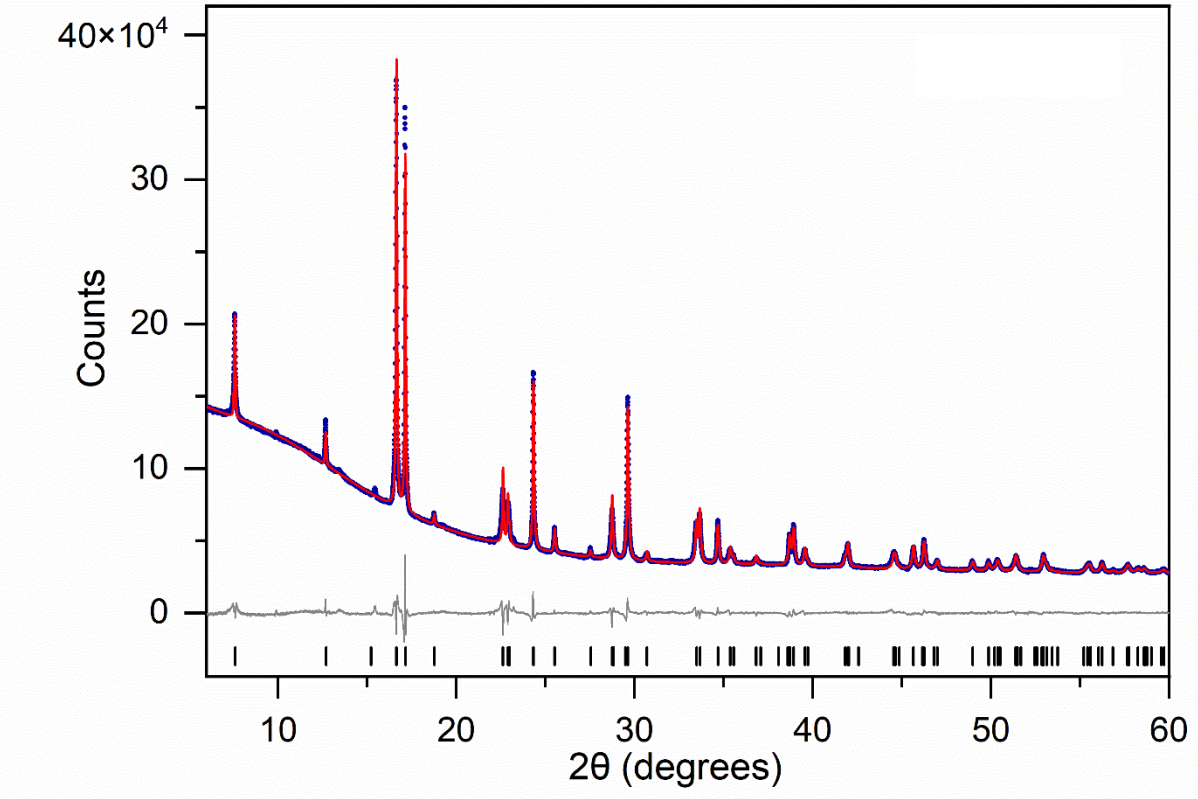


**Figure S1.** Observed, calculated and difference plots from the structural refinement of $Sr_2Co_{0.5}Ir_{0.5}O_4$ against SXRD data collected at room temperature.

| **$Sr_2Co_{0.5}Ir_{0.5}O_4$, space group *I4/mmm* (No. 139)** | | | | | | |
|---|---|---|---|---|---|---|
| | | ***x*** | ***y*** | ***z*** | **Occ.** | **$B_{iso}$ (Å$^2$)** |
| Sr(1) | 4*e* | 0 | 0 | 0.35550(7) | 1 | 0.46(3) |
| Co(1)/Ir(1) | 2*a* | 0 | 0 | 0 | 0.5/0.5 | 0.27(3) |
| O(1) | 4*c* | 0 | ½ | 0 | 1 | 1.19(7) |
| O(2) | 4*e* | 0 | 0 | 0.1604(3) | 1 | 1.19(7) |
| $a$ = 3.91778(6) Å, $c$ = 12.4770(2) Å | | | | | | |
| $V$ = 191.510(7) Å$^3$, $Z$ = 2 | | | | | | |
| Formula weight = 364.8 g mol$^{-1}$ | | | | | | |
| Radiation source: Synchrotron X-ray radiation ($\lambda$ = 0.825 Å), Temperature = 298 K | | | | | | |
| $R_{wp}$ = 2.26%, $R_p$ = 1.38%, *gof* = 5.31 | | | | | | |

**Table S1.** Parameters from the structural refinement of $Sr_2Co_{0.5}Ir_{0.5}O_4$ against SXRD data collected at room temperature.

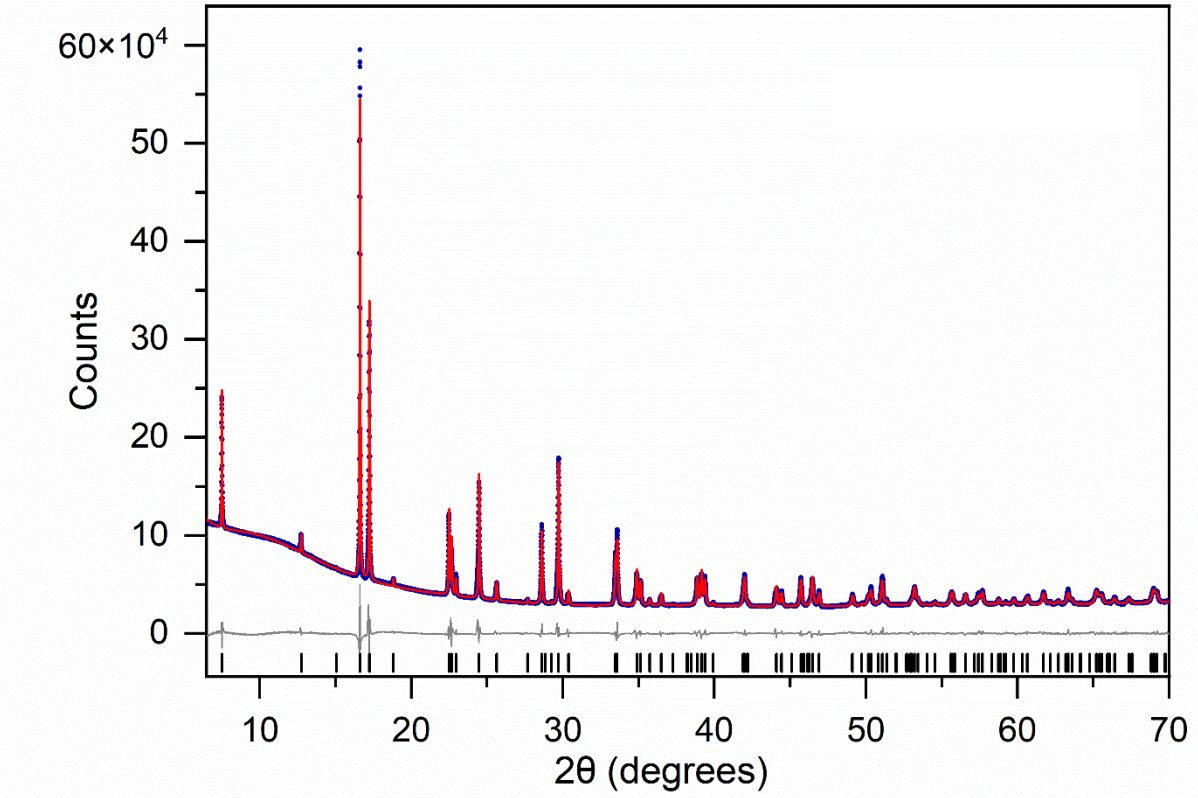


**Figure S2.** Observed, calculated and difference plots from the structural refinement of $La_{0.25}Sr_{1.75}Co_{0.5}Ir_{0.5}O_4$ against SXRD data collected at room temperature.

| **$La_{0.25}Sr_{1.75}Co_{0.5}Ir_{0.5}O_4$, space group *I4/mmm* (No. 139)** | | | | | | |
|---|---|---|---|---|---|---|
| | | ***x*** | ***y*** | ***z*** | **Occ.** | **$B_{iso}$ (Å$^2$)** |
| La(1)/Sr(1) | 4*e* | 0 | 0 | 0.35622(4) | 0.125/0.875 | 0.77(2) |
| Co(1)/Ir(1) | 2*a* | 0 | 0 | 0 | 0.5/0.5 | 0.46(2) |
| O(1) | 4*c* | 0 | ½ | 0 | 1 | 1.07(5) |
| O(2) | 4*e* | 0 | 0 | 0.1647(4) | 1 | 1.07(5) |
| $a$ = 3.88836(3) Å, $c$ = 12.5844(1) Å | | | | | | |
| $V$ = 190.268(4) Å$^3$, $Z$ = 2 | | | | | | |
| Formula weight = 377.64 g mol$^{-1}$ | | | | | | |
| Radiation source: Synchrotron X-ray radiation ($\lambda$ = 0.825 Å), Temperature = 298 K | | | | | | |
| $R_{wp}$ = 2.93%, $R_p$ = 1.76%, *gof* = 6.22 | | | | | | |

**Table S2.** Parameters from the structural refinement of $La_{0.25}Sr_{1.75}Co_{0.5}Ir_{0.5}O_4$ against SXRD data collected at room temperature.

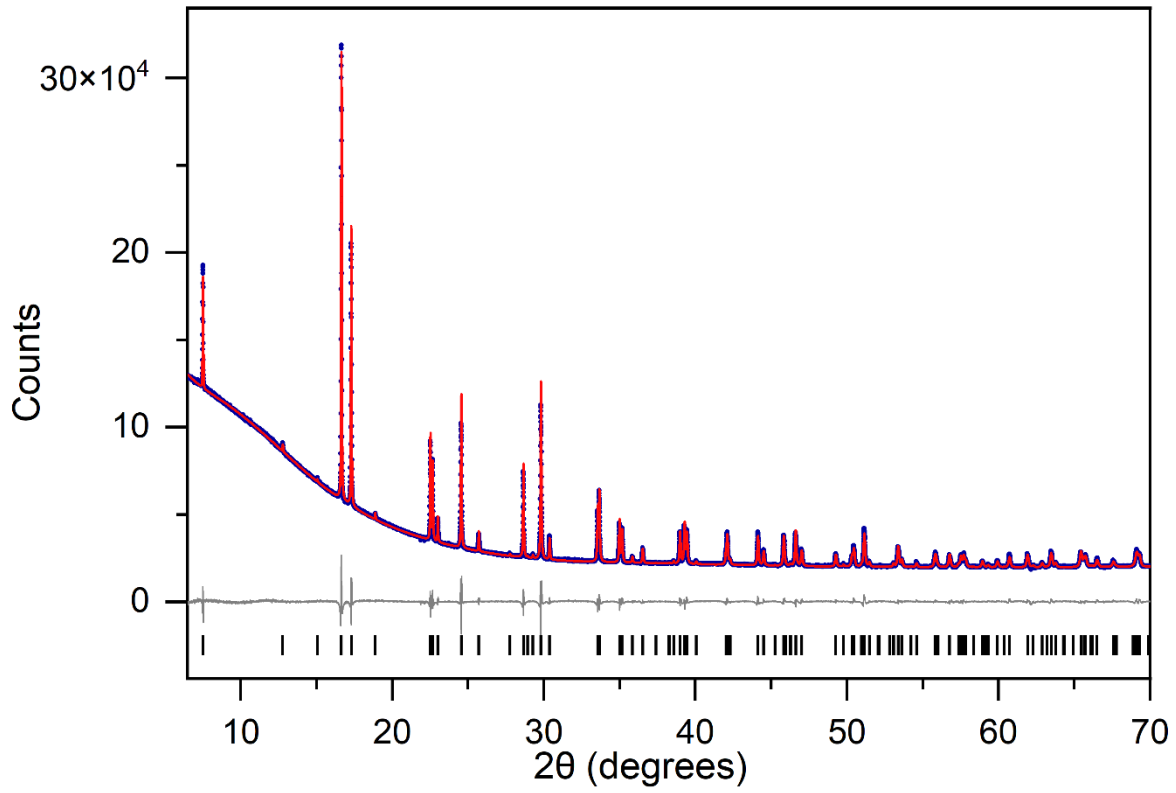


**Figure S3.** Observed, calculated and difference plots from the structural refinement of $La_{0.5}Sr_{1.5}Co_{0.5}Ir_{0.5}O_4$ against SXRD data collected at room temperature.

| **$La_{0.5}Sr_{1.5}Co_{0.5}Ir_{0.5}O_4$, space group *I*4/*mmm* (No. 139)** | | | | | | |
|---|---|---|---|---|---|---|
| | | ***x*** | ***y*** | ***z*** | **Occ.** | **$B_{iso}$ (Å$^2$)** |
| La(1)/Sr(1) | 4*e* | 0 | 0 | 0.35697(4) | 0.25/0.75 | 0.72(2) |
| Co(1)/Ir(1) | 2*a* | 0 | 0 | 0 | 0.5/0.5 | 0.58(2) |
| O(1) | 4*c* | 0 | ½ | 0 | 1 | 1.28(6) |
| O(2) | 4*e* | 0 | 0 | 0.1649(6) | 1 | 1.28(6) |
| $a$ = 3.87999(4) Å, $c$ = 12.5927(1) Å | | | | | | |
| $V$ = 189.574(4) Å$^3$, $Z$ = 2 | | | | | | |
| Formula weight = 390.45 g mol$^{-1}$ | | | | | | |
| Radiation source: Synchrotron X-ray radiation ($\lambda$ = 0.825 Å), Temperature = 298 K | | | | | | |
| $R_{wp}$ = 2.20%, $R_p$ = 1.16%, *gof* = 4.28 | | | | | | |

**Table S3.** Parameters from the structural refinement of $La_{0.5}Sr_{1.5}Co_{0.5}Ir_{0.5}O_4$ against SXRD data collected at room temperature.

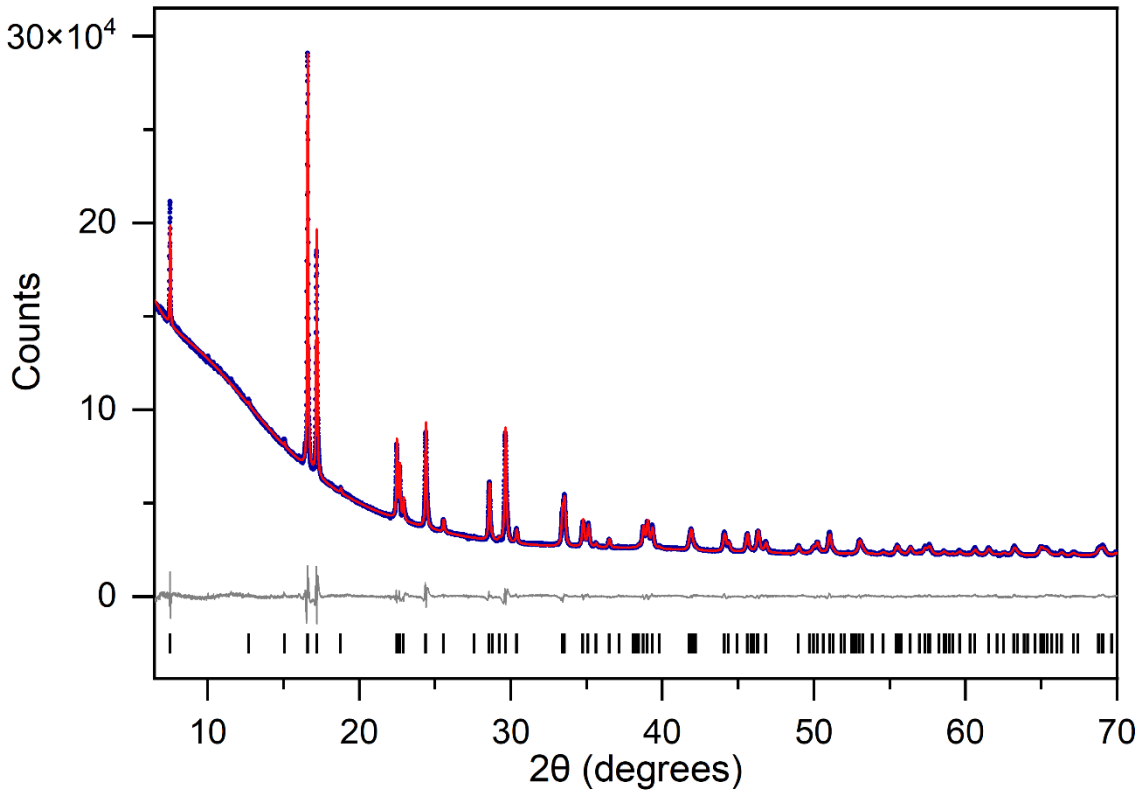


**Figure S4.** Observed, calculated and difference plots from the structural refinement of $La_{0.75}Sr_{1.25}CoIrO_4$ against SXRD data collected at room temperature.

| **$La_{0.75}Sr_{1.25}CoIrO_4$, space group *I*4/*mmm* (No. 139)** | | | | | | |
|---|---|---|---|---|---|---|
| | | ***x*** | ***y*** | ***z*** | **Occ.** | **$B_{iso}$ (Å$^2$)** |
| La(1)/Sr(1) | 4*e* | 0 | 0 | 0.35744(5) | 0.375/0.625 | 1.51(2) |
| Co(1)/Ir(1) | 2*a* | 0 | 0 | 0 | 0.5/0.5 | 1.16(2) |
| O(1) | 4*c* | 0 | ½ | 0 | 1 | 2.03(7) |
| O(2) | 4*e* | 0 | 0 | 0.1641(6) | 1 | 2.03(7) |
| $a$ = 3.90328(7) Å, $c$ = 12.5893(2) Å | | | | | | |
| $V$ = 191.805(8) Å$^3$, $Z$ = 2 | | | | | | |
| Formula weight = 403.28 g mol$^{-1}$ | | | | | | |
| Radiation source: Synchrotron X-ray radiation ($\lambda$ = 0.825 Å), Temperature = 298 K | | | | | | |
| $R_{wp}$ = 1.85%, $R_p$ = 1.11%, *gof* = 3.01 | | | | | | |

**Table S4.** Parameters from the structural refinement of $La_{0.75}Sr_{1.25}CoIrO_4$ against SXRD data collected at room temperature.

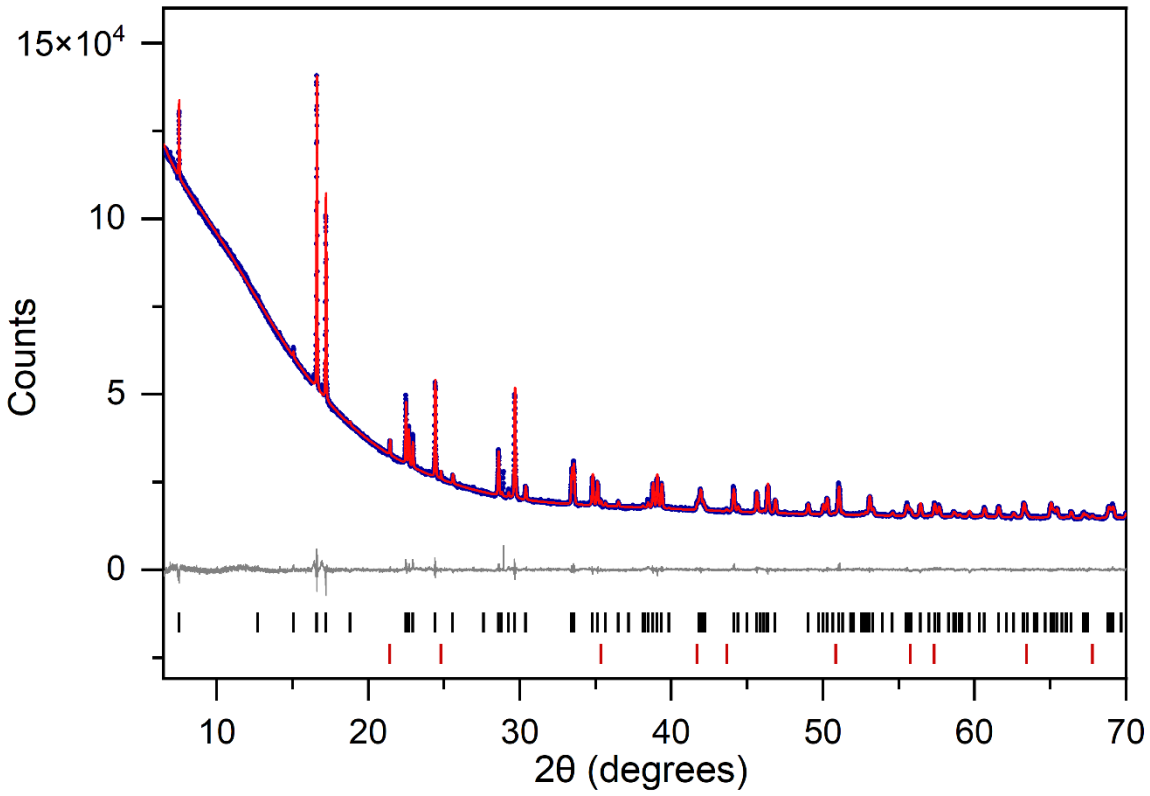


**Figure S5.** Observed, calculated and difference plots from the structural refinement of $LaSrCo_{0.5}Ir_{0.5}O_4$ against SXRD data collected at room temperature. Upper tick marks indicate peak positions of the main phase, lower tick marks a secondary phase of Ir metal.

| **$LaSrCo_{0.5}Ir_{0.5}O_4$, space group *I*4/*mmm* (No. 139), 98.70(5) wt%** | | | | | | |
|---|---|---|---|---|---|---|
| | | ***x*** | ***y*** | ***z*** | **Occ.** | **$B_{iso}$ (Å²)** |
| La(1)/Sr(1) | 4*e* | 0 | 0 | 0.35939(4) | 0.5/0.5 | 0.49(1) |
| Co(1)/Ir(1) | 2*a* | 0 | 0 | 0 | 0.5/0.5 | 1.21(1) |
| O(1) | 4*c* | 0 | ½ | 0 | 1 | 0.84(5) |
| O(2) | 4*e* | 0 | 0 | 0.1645(6) | 1 | 0.84(5) |
| $a$ = 3.89677(2) Å, $c$ = 12.5777(1) Å | | | | | | |
| $V$ = 190.990(3) Å³, $Z$ = 2 | | | | | | |
| Formula weight = 416.1 g mol$^{-1}$ | | | | | | |
| **Ir, space group *Fm*$\bar{3}$*m* (No. 225), 1.30(5) wt%** | | | | | | |
| | | ***x*** | ***y*** | ***z*** | **Occ.** | **$B_{iso}$ (Å²)** |
| Ir(1) | 4*a* | 0 | 0 | 0 | 1 | 0.17(7) |
| $a$ = 3.8386(1) Å | | | | | | |
| $V$ = 56.562(7) Å³, $Z$ = 4 | | | | | | |
| Formula weight = 192.22 g mol$^{-1}$ | | | | | | |
| Radiation source: Synchrotron X-ray radiation ($\lambda$ = 0.825 Å), Temperature = 298 K | | | | | | |
| $R_{wp}$ = 1.12%, $R_p$ = 0.73%, *gof* = 1.98 | | | | | | |

**Table S5.** Parameters from the structural refinement of $LaSrCo_{0.5}Ir_{0.5}O_4$ against SXRD data collected at room temperature.

## 2. Thermogravimetric data from $La_xSr_{2-x}Co_{0.5}Ir_{0.5}O_{4-y}H_z$ phases.

As can be seen from the data in Figures S6-S10, the oxidation of samples only occurs at a significant rate on heating. Samples are not observed to oxidize on exposure to air at room temperature for 5 minutes. However, all samples were treated as air-sensitive as a precaution. We expect the samples to slowly oxidize over a period of hours/days at room temperature.

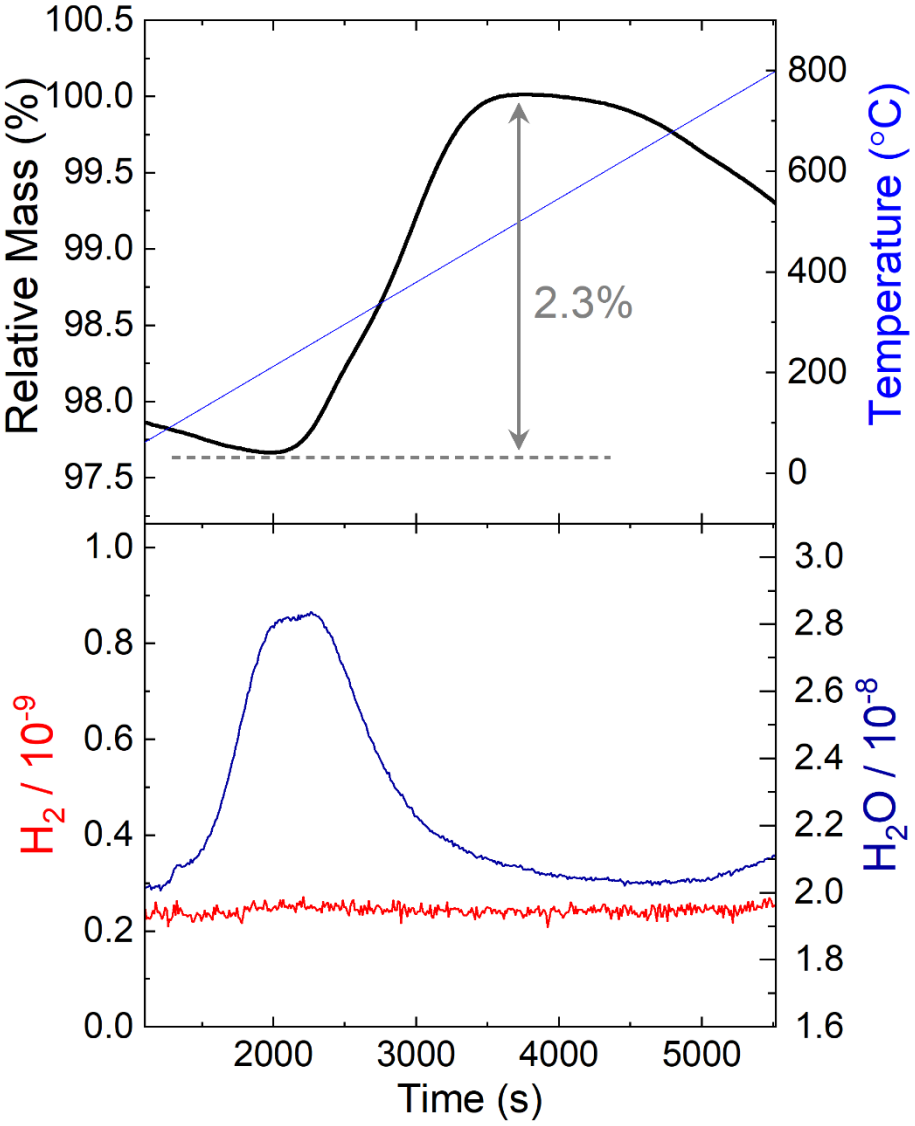


**Figure S6.** Thermogravimetric data (top) and m/z = 18 and m/z = 2 mass-spectrum signals (bottom) collected as a function of temperature while heating $Sr_2Co_{0.5}Ir_{0.5}O_{4-y}H_z$ under flowing oxygen.

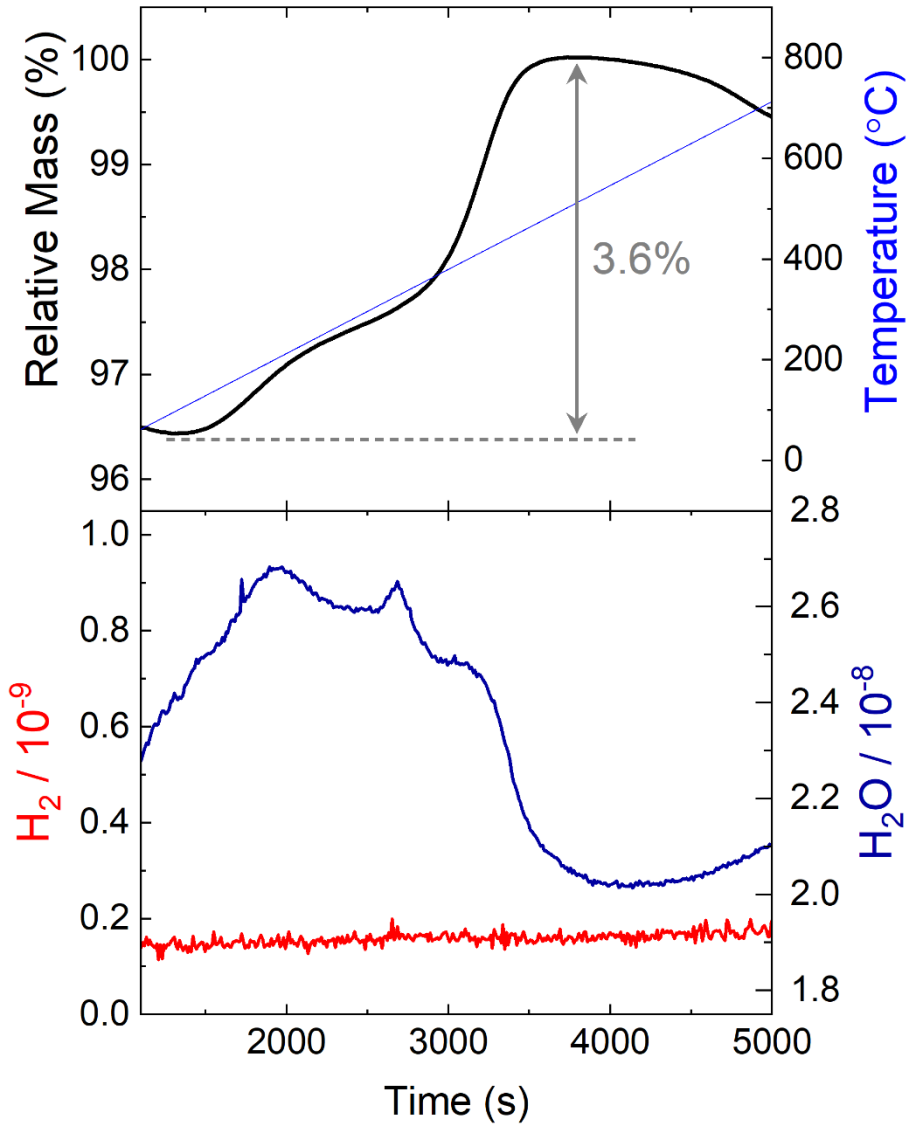


**Figure S7.** Thermogravimetric data (top) and m/z = 18 and m/z = 2 mass-spectrum signals (bottom) collected as a function of temperature while heating $La_{0.25}Sr_{1.75}Co_{0.5}Ir_{0.5}O_{4-y}H_z$ under flowing oxygen.

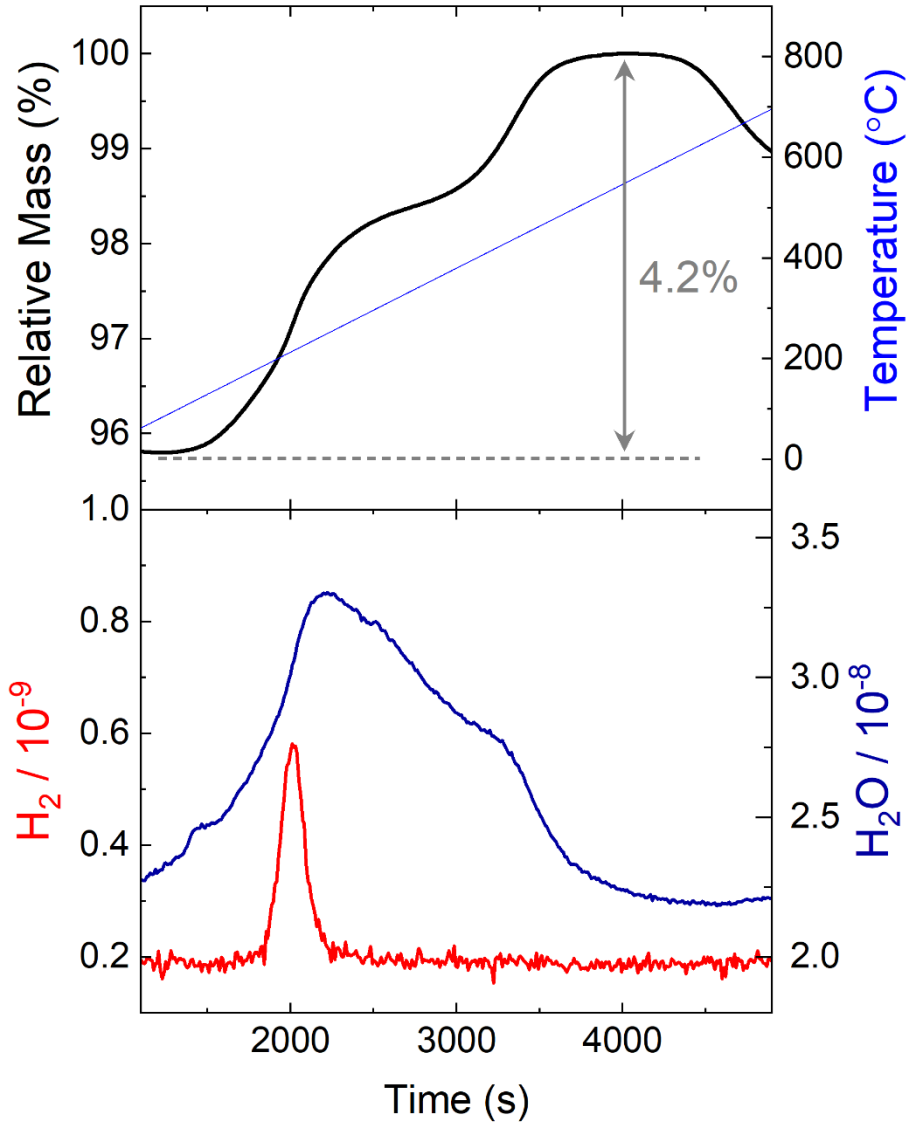


**Figure S8.** Thermogravimetric data (top) and m/z = 18 and m/z = 2 mass-spectrum signals (bottom) collected as a function of temperature while heating $La_{0.5}Sr_{1.5}Co_{0.5}Ir_{0.5}O_{4-y}H_z$ under flowing oxygen.

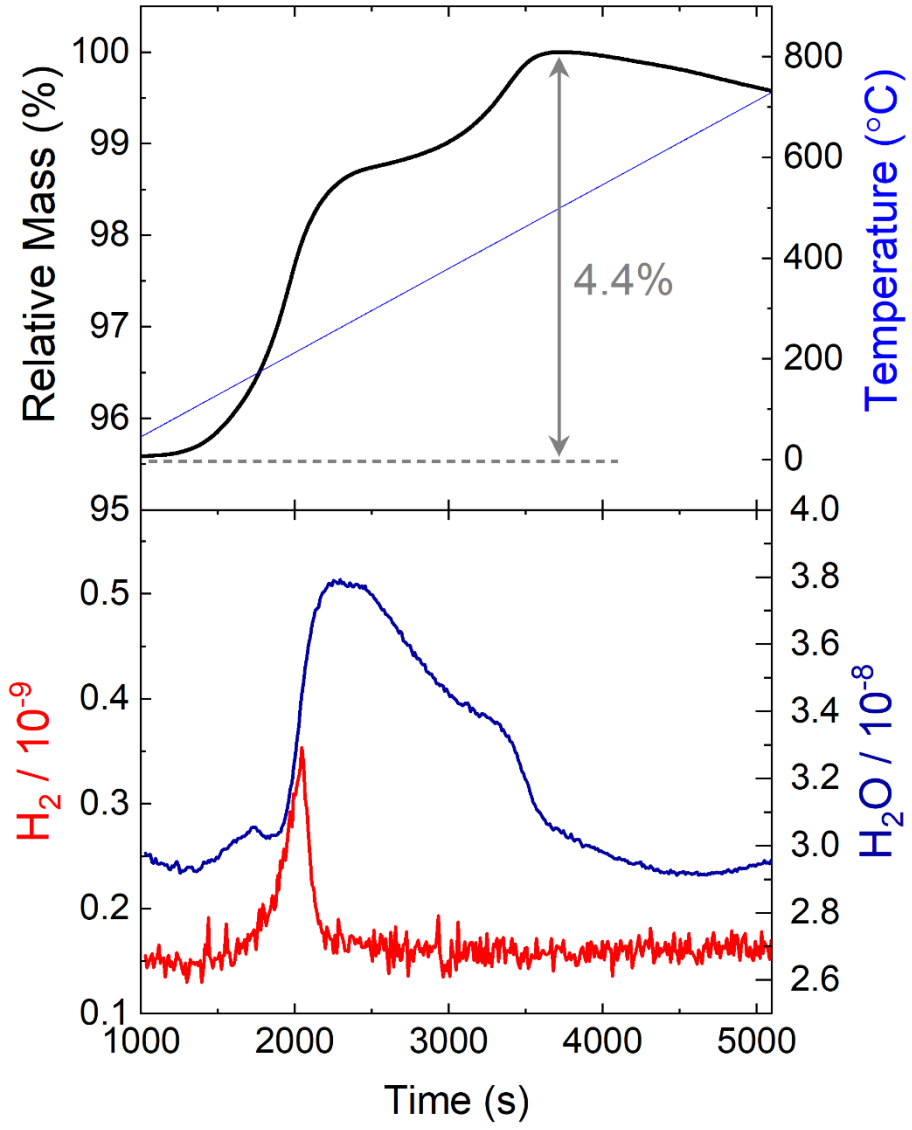


**Figure S9.** Thermogravimetric data (top) and m/z = 18 and m/z = 2 mass-spectrum signals (bottom) collected as a function of temperature while heating $La_{0.75}Sr_{1.25}Co_{0.5}Ir_{0.5}O_{4-y}H_z$ under flowing oxygen.

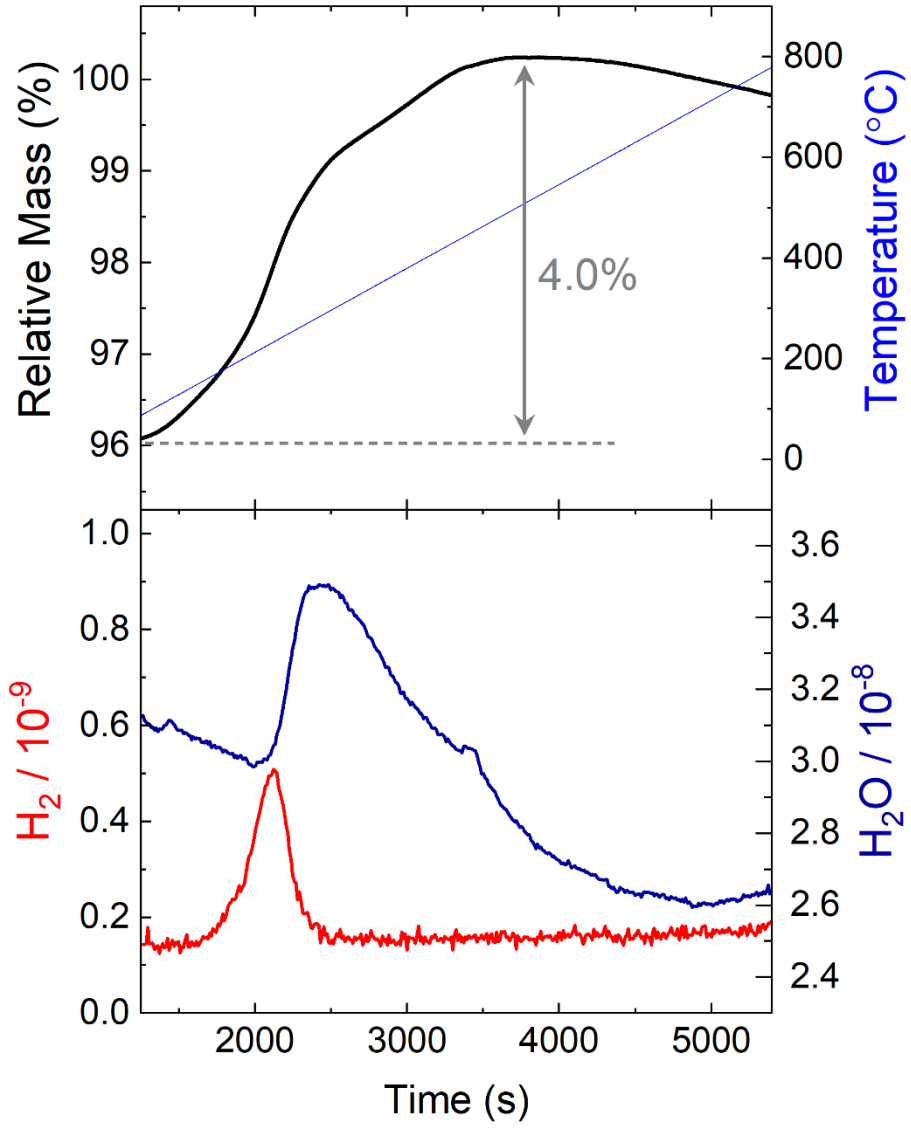


**Figure S10.** Thermogravimetric data (top) and m/z = 18 and m/z = 2 mass-spectrum signals (bottom) collected as a function of temperature while heating $LaSrCo_{0.5}Ir_{0.5}O_{4-y}H_z$ under flowing oxygen.

## 2. Structural characterization of $La_xSr_{2-x}Co_{0.5}Ir_{0.5}O_{4-y}H_z$ ($x$ = 0, 0.25, 0.5, 0.75, 1) phases.

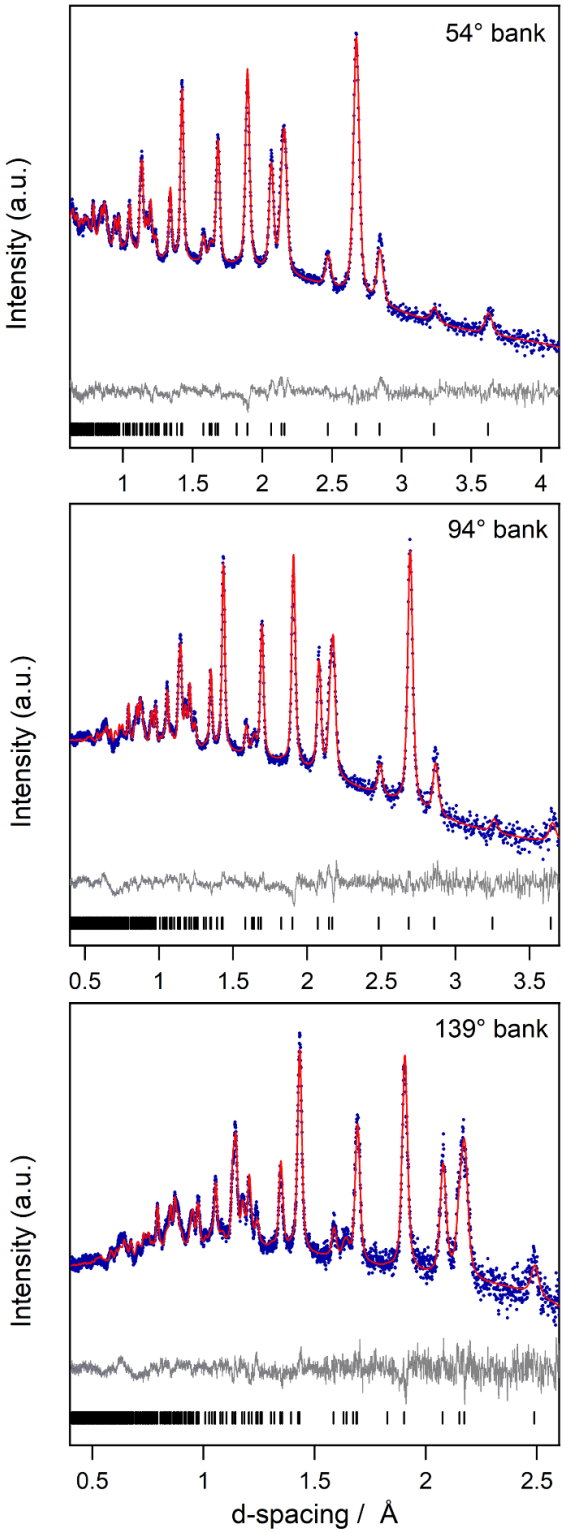


**Figure S11.** Observed, calculated and difference plots from the structural refinement of $Sr_2Co_{0.5}Ir_{0.5}O_{3.25}H_{0.75}$ against NPD data collected at room temperature from the 3 different detector banks of the POLARIS instrument.

| $Sr_2Co_{0.5}Ir_{0.5}O_{3.27(1)}H_{0.73(1)}$, space group *I*4/*mmm* (No. 139) | | | | | | |
|---|---|---|---|---|---|---|
| | | ***x*** | ***y*** | ***z*** | **Occ.** | $B_{iso}$ (Å$^2$) |
| Sr(1) | 4*e* | 0 | 0 | 0.3530(1) | 1 | 1.18(4) |
| Co(1)/Ir(1) | 2*a* | 0 | 0 | 0 | 0.5/0.5 | 1.44(6) |
| O(1)/H(1) | 4*c* | 0 | ½ | 0 | 0.635(3)/0.365(3) | 1.05(8) |
| O(2) | 4*e* | 0 | 0 | 0.1629(2) | 1 | 1.60(6) |
| $a$ = 3.8058(3) Å, $c$ = 13.037(1) Å | | | | | | |
| $V$ = 188.84(4) Å$^3$, $Z$ = 2 | | | | | | |
| Formula weight = 353.87 g mol$^{-1}$ | | | | | | |
| Radiation source: time-of-flight neutrons, Temperature = 298 K | | | | | | |
| $R_{wp}$ = 2.11%, $R_p$ = 1.63%, *gof* = 0.06 | | | | | | |

**Table S6.** Parameters from the structural refinement of $Sr_2Co_{0.5}Ir_{0.5}O_{3.25}H_{0.75}$ against NPD data collected at room temperature.

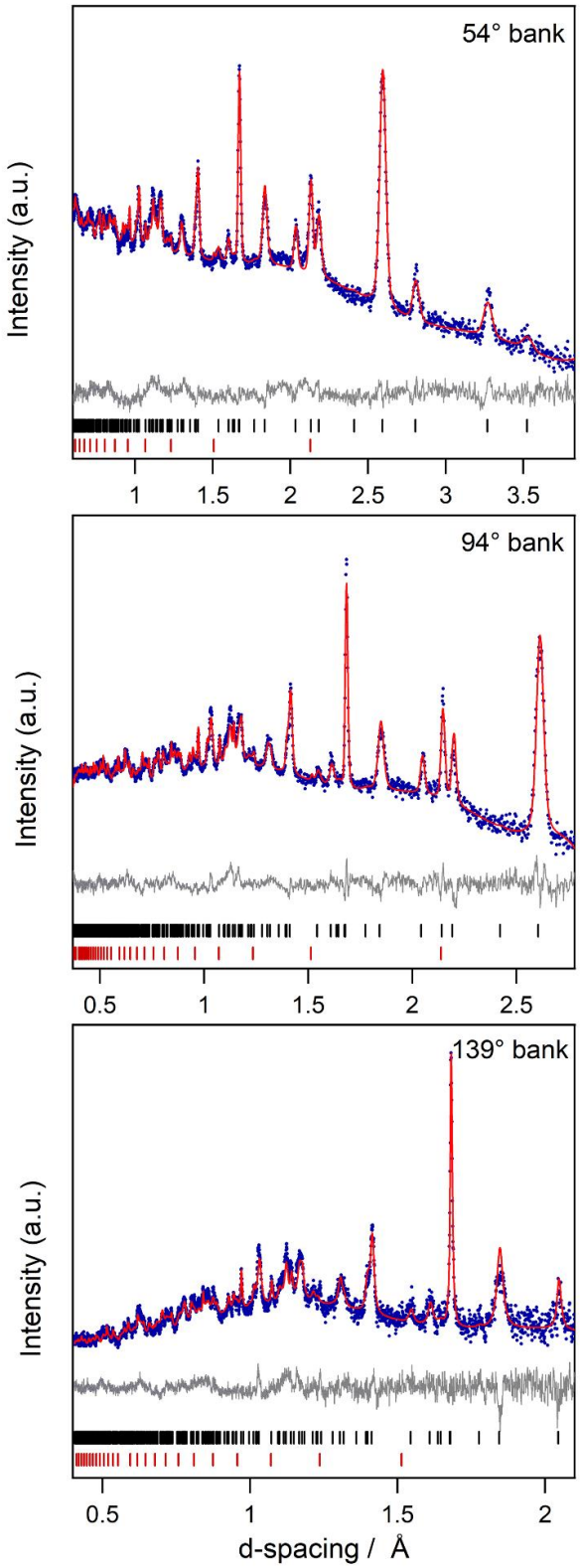


**Figure S12.** Observed, calculated and difference plots from the structural refinement of $La_{0.25}Sr_{1.75}CoIrO_{2.75}H_{1.25}$ against NPD data collected at room temperature from the 3 different detector banks of the POLARIS instrument. Upper tick marks indicate peak positions of $La_{0.25}Sr_{1.75}CoIrO_{2.75}H_{1.25}$ lower tick marks from the vanadium sample holder.

| $La_{0.25}Sr_{1.75}Co_{0.5}Ir_{0.5}O_{2.74(1)}H_{1.26(1)}$, space group *I*4/*mmm* (No. 139) | | | | | | |
|---|---|---|---|---|---|---|
| | | ***x*** | ***y*** | ***z*** | **Occ.** | $B_{iso}$ **(Å²)** |
| La(1)/Sr(1) | 4*e* | 0 | 0 | 0.3523(1) | 0.125/0.875 | 0.14(4) |
| Co(1)/Ir(1) | 2*a* | 0 | 0 | 0 | 0.5/0.5 | 0.69(7) |
| O(1)/H(1) | 4*c* | 0 | ½ | 0 | 0.369(3)/0.631(3) | 0.23(6) |
| O(2) | 4*e* | 0 | 0 | 0.1624(2) | 1 | 0.23(6) |
| $a$ = 3.6888(5) Å, $c$ = 13.172(1) Å | | | | | | |
| $V$ = 179.23(5) Å$^3$ | | | | | | |
| Formula weight = 358.75 g mol$^{-1}$ | | | | | | |
| Radiation source: time-of-flight neutrons, Temperature = 298 K | | | | | | |
| $R_{wp}$ = 1.84%, $R_p$ = 1.41%, *gof* = 0.03 | | | | | | |

**Table S7.** Parameters from the structural refinement of $La_{0.25}Sr_{1.75}CoIrO_{2.75}H_{1.25}$ against NPD data collected at room temperature.

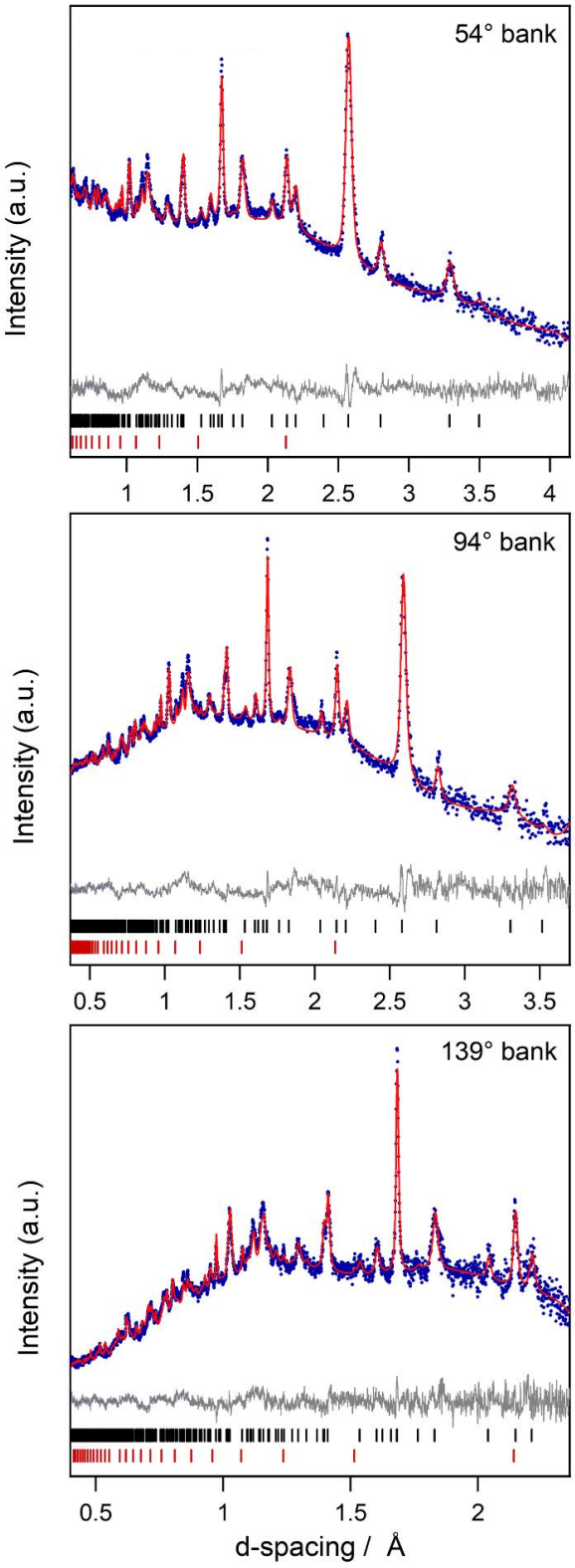


**Figure S13.** Observed, calculated and difference plots from the structural refinement of $La_{0.5}Sr_{1.5}CoIrO_{2.5}H_{1.5}$ against NPD data collected at room temperature from the 3 different detector banks of the POLARIS instrument. Upper tick marks indicate peak positions of $La_{0.5}Sr_{1.5}CoIrO_{2.5}H_{1.5}$ lower tick marks from the vanadium sample holder.

| $La_{0.5}Sr_{1.5}Co_{0.5}Ir_{0.5}O_{2.50(1)}H_{1.50(1)}$, space group *I*4/*mmm* (No. 139) | | | | | | |
|---|---|---|---|---|---|---|
| | | ***x*** | ***y*** | ***z*** | **Occ.** | $B_{iso}$ (Å$^2$) |
| La(1)/Sr(1) | 4*e* | 0 | 0 | 0.3529(2) | 0.25/0.75 | 0.08(4) |
| Co(1)/Ir(1) | 2*a* | 0 | 0 | 0 | 0.5/0.5 | 1.1(1) |
| O(1)/H(1) | 4*c* | 0 | ½ | 0 | 0.253(4)/0.747(4) | 0.35(6) |
| O(2) | 4*e* | 0 | 0 | 0.1656(3) | 1 | 0.35(6) |
| *a* = 3.6596(5) Å, *c* = 13.266(2) Å | | | | | | |
| *V* = 177.67(6) Å$^3$, *Z* = 2 | | | | | | |
| Formula weight = 368.05 g mol$^{-1}$ | | | | | | |
| Radiation source: time-of-flight neutrons, Temperature = 298 K | | | | | | |
| $R_{wp}$ = 1.67%, $R_p$ = 1.29%, *gof* = 0.05 | | | | | | |

**Table S8.** Parameters from the structural refinement of $La_{0.5}Sr_{1.5}CoIrO_{2.5}H_{1.5}$ against NPD data collected at room temperature.

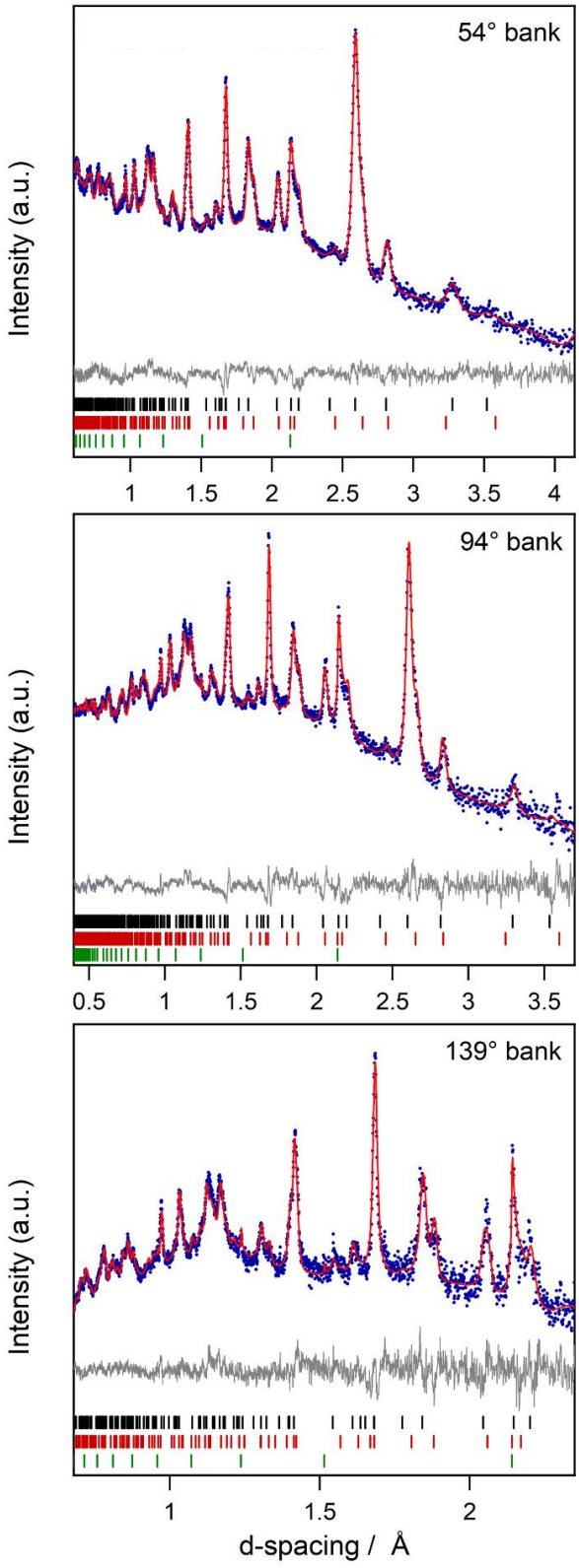


**Figure S14.** Observed, calculated and difference plots from the structural refinement of $La_{0.75}Sr_{1.25}CoIrO_{2.75}H_{1.25}$ against NPD data collected at room temperature from the 3 different detector banks of the POLARIS instrument. Upper tick marks indicate peak positions of majority phase ($La_{0.75}Sr_{1.25}CoIrO_{2.75}H_{1.25}$), middle tick marks the minority phase ($La_{0.75}Sr_{1.25}CoIrO_{3.4}H_{0.6}$), lower tick marks from the vanadium sample holder.

| $La_{0.75}Sr_{1.25}Co_{0.5}Ir_{0.5}O_{2.73(2)}H_{1.27(2)}$, space group *I*4/*mmm* (No. 139), 85.3(8) wt% | | | | | | |
|---|---|---|---|---|---|---|
| | | ***x*** | ***y*** | ***z*** | **Occ.** | $B_{iso}$ (Å$^2$) |
| La(1)/Sr(1) | 4*e* | 0 | 0 | 0.3547(2) | 0.625/0.375 | 0.1(2) |
| Co(1)/Ir(1) | 2*a* | 0 | 0 | 0 | 0.5/0.5 | 2.5(2) |
| O(1)/H(1) | 4*c* | 0 | ½ | 0 | 0.367(4)/0.633(4) | 0.16(2) |
| O(2) | 4*e* | 0 | 0 | 0.1692(3) | 1 | 0.16(2) |
| *a* = 3.6895(7) Å, *c* = 13.233(2) Å | | | | | | |
| *V* = 180.13(7) Å$^3$, *Z* = 2 | | | | | | |
| Formula weight = 384.32 g mol$^{-1}$ | | | | | | |
| $La_{0.75}Sr_{1.25}Co_{0.5}Ir_{0.5}O_{3.39(3)}H_{0.61(3)}$, space group *I*4/*mmm* (No. 139), 14.7(7) wt% | | | | | | |
| | | ***x*** | ***y*** | ***z*** | **Occ.** | $B_{iso}$ (Å$^2$) |
| La(1)/Sr(1) | 4*e* | 0 | 0 | 0.3547(2) | 0.625/0.375 | 0.1(2) |
| Co(1)/Ir(1) | 2*a* | 0 | 0 | 0 | 0.5/0.5 | 2.5(5) |
| O(1)/H(1) | 4*c* | 0 | ½ | 0 | 0.70(1)/0.30(1) | 0.16(2) |
| O(2) | 4*e* | 0 | 0 | 0.1692(3) | 1 | 0.16(2) |
| *a* = 3.7661(8) Å, *c* = 13.029(5) Å | | | | | | |
| *V* = 184.8(1) Å$^3$ | | | | | | |
| Formula weight = 394.21 g mol$^{-1}$ | | | | | | |
| Radiation source: time-of-flight neutrons, Temperature = 298 K | | | | | | |
| $R_{wp}$ = 1.81%, $R_p$ = 1.40%, *gof* = 0.04 | | | | | | |

**Table S9.** Parameters from the 2-phase structural refinement of $La_{0.75}Sr_{1.25}CoIrO_{2.75}H_{1.25}$ and $La_{0.75}Sr_{1.25}CoIrO_{3.4}H_{0.6}$ against NPD data collected at room temperature. The displacement parameters of analogous atoms were constrained to be the same in the two phases.

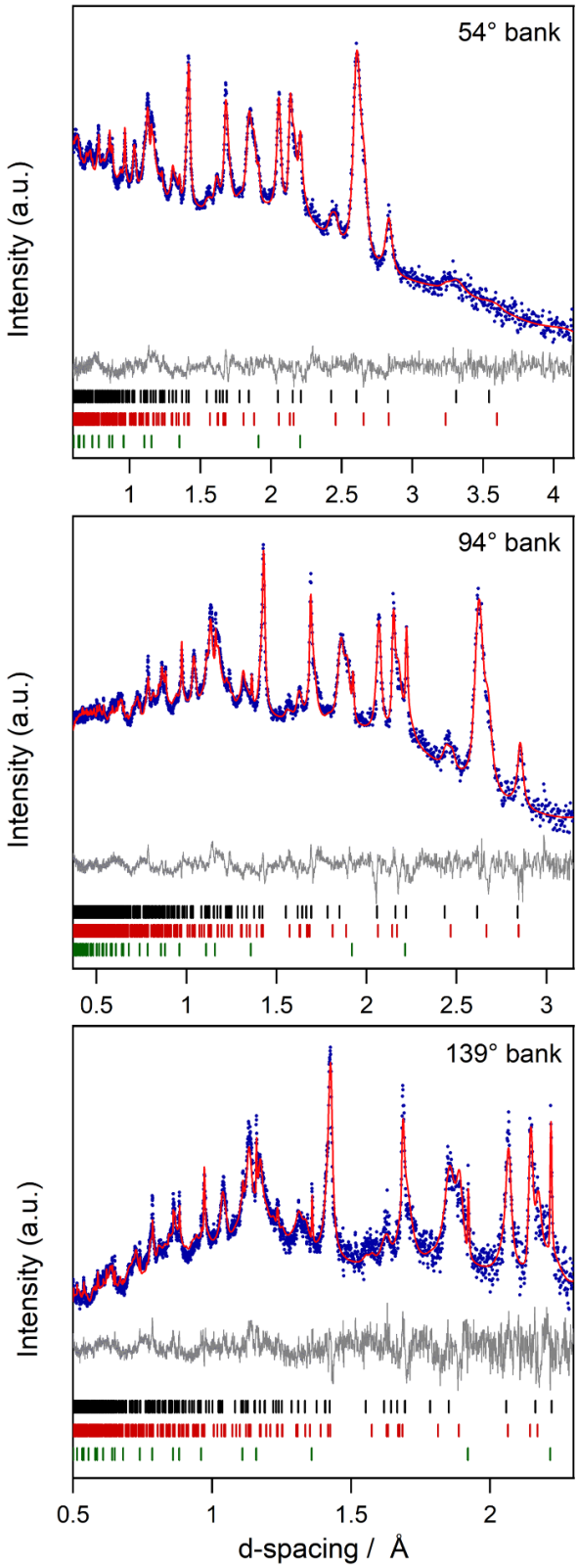


**Figure S15.** Observed, calculated and difference plots from the structural refinement of $LaSrCo_{0.5}Ir_{0.5}O_3H$ against NPD data collected at room temperature from the 3 different detector banks of the POLARIS instrument. Upper tick marks indicate peak positions of majority phase ($LaSrCo_{0.5}Ir_{0.5}O_3H$), middle tick marks the minority phase ($LaSrCo_{0.5}Ir_{0.5}O_{3.5}H_{0.5}$), lower tick marks from the vanadium sample holder.

| **$LaSrCo_{0.5}Ir_{0.5}O_{3.00(3)}H_{1.00(3)}$, space group *I*4/*mmm* (No. 139), 83.6(8) wt%** | | | | | | |
|---|---|---|---|---|---|---|
| | | ***x*** | ***y*** | ***z*** | **Occ.** | **$B_{iso}$ (Å²)** |
| La(1)/Sr(1) | 4*e* | 0 | 0 | 0.3529(4) | 0.5/0.5 | 0.36(8) |
| Co(1)/Ir(1) | 2*a* | 0 | 0 | 0 | 0.5/0.5 | 2.95(4) |
| O(1)/H(1) | 4*c* | 0 | ½ | 0 | 0.50(2)/0.50(2) | 0.34(2) |
| O(2) | 4*e* | 0 | 0 | 0.1696(4) | 1 | 0.34(3) |
| *a* = 3.7070(6) Å, *c* = 13.342(4) Å | | | | | | |
| *V* = 183.35(8) Å³, *Z* = 2 | | | | | | |
| Formula weight = 401.04 g mol$^{-1}$ | | | | | | |
| **$LaSrCo_{0.5}Ir_{0.5}O_{3.48(3)}H_{0.52(3)}$, space group *I*4/*mmm* (No. 139), 16.4(8) wt%** | | | | | | |
| | | ***x*** | ***y*** | ***z*** | **Occ.** | **$B_{iso}$ (Å²)** |
| La(1)/Sr(1) | 4*e* | 0 | 0 | 0.3606(4) | 0.5/0.5 | 0.36(8) |
| Co(1)/Ir(1) | 2*a* | 0 | 0 | 0 | 0.5/0.5 | 2.95(4) |
| O(1)/H(1) | 4*c* | 0 | ½ | 0 | 0.74(1)/0.26(1) | 0.34(2) |
| O(2) | 4*e* | 0 | 0 | 0.1719(6) | 1 | 0.34(3) |
| *a* = 3.7789(8) Å, *c* = 13.040(2) Å | | | | | | |
| *V* = 186.21(9) Å³, *Z* = 2 | | | | | | |
| Formula weight = 408.38 g mol$^{-1}$ | | | | | | |
| Radiation source: time-of-flight neutrons, Temperature = 298 K | | | | | | |
| $R_{wp}$ = 1.80%, $R_p$ = 1.41%, *gof* = 0.04 | | | | | | |

**Table S10.** Parameters from the 2-phase structural refinement of $LaSrCo_{0.5}Ir_{0.5}O_3H$ and $LaSrCo_{0.5}Ir_{0.5}O_{3.5}H_{0.5}$ against NPD data collected at room temperature. The displacement parameters of analogous atoms were constrained to be the same in the two phases.

## 4. Magnetic characterization of $La_xSr_{2-x}Co_{0.5}Ir_{0.5}O_{4-y}H_y$ phases.

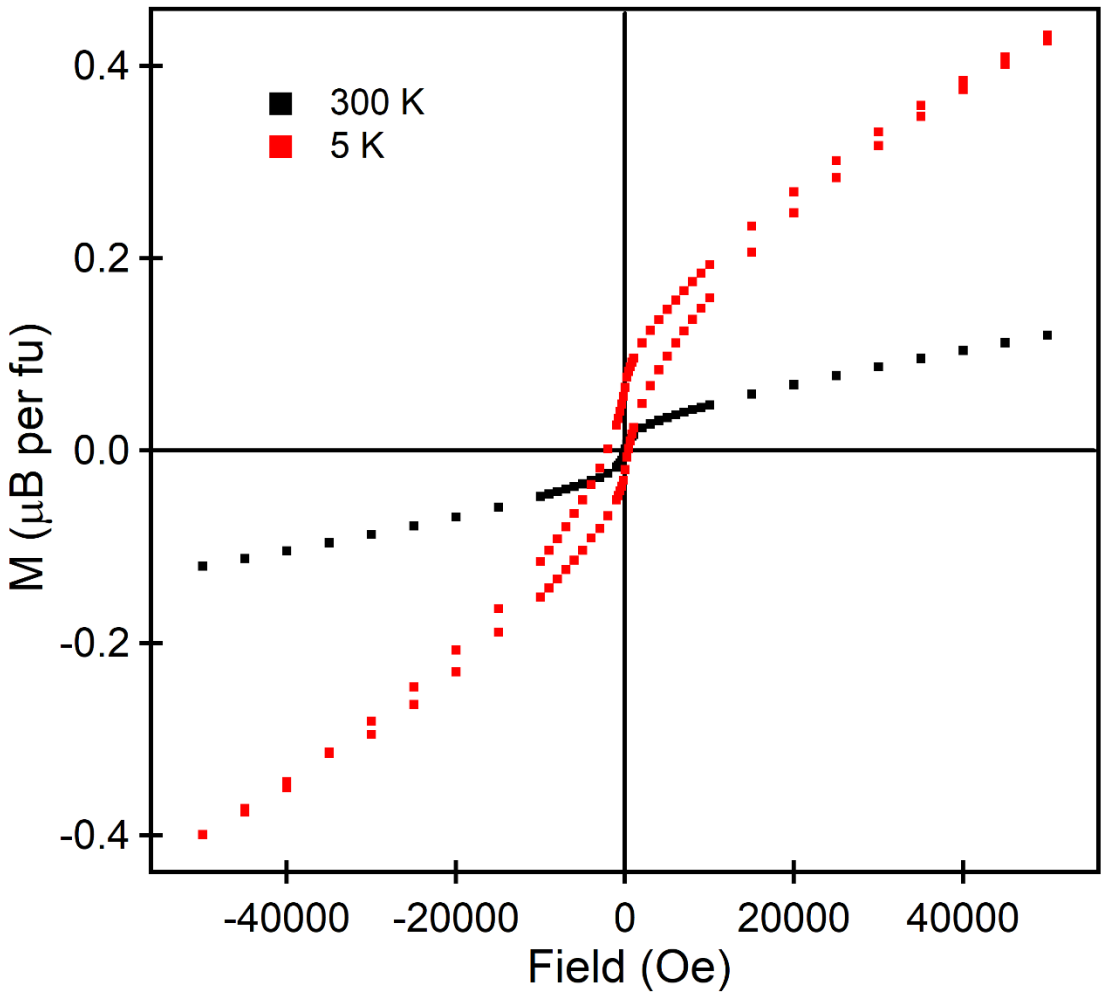


**Figure S16.** Magnetization-field data collected from $Sr_2Co_{0.5}Ir_{0.5}O_{3.25}H_{0.75}$ at 300 K and at 5 K after cooling from 300 K in an applied field of 5 T.

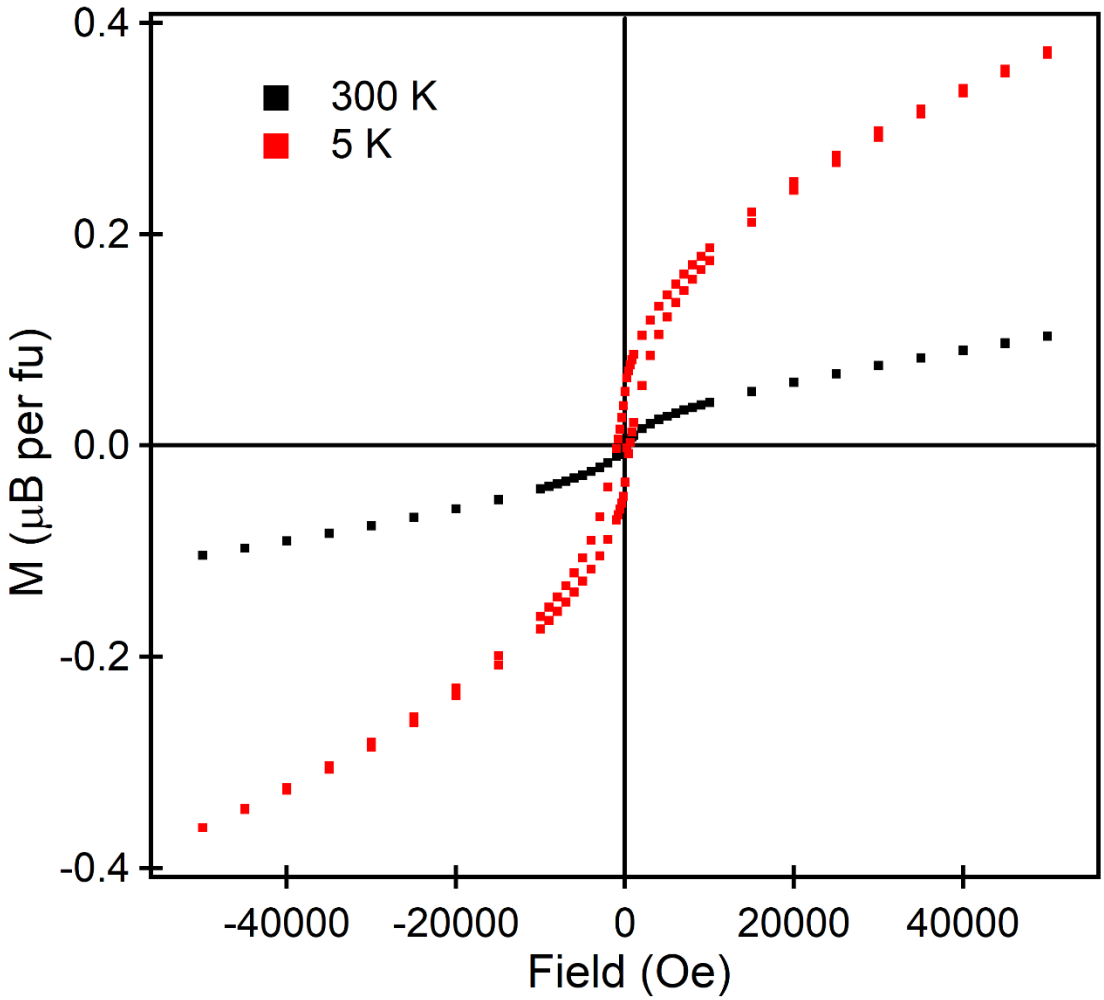


**Figure S17.** Magnetization-field data collected from $La_{0.25}Sr_{1.75}CoIrO_{2.75}H_{1.25}$ at 300 K and at 5 K after cooling from 300 K in an applied field of 5 T.

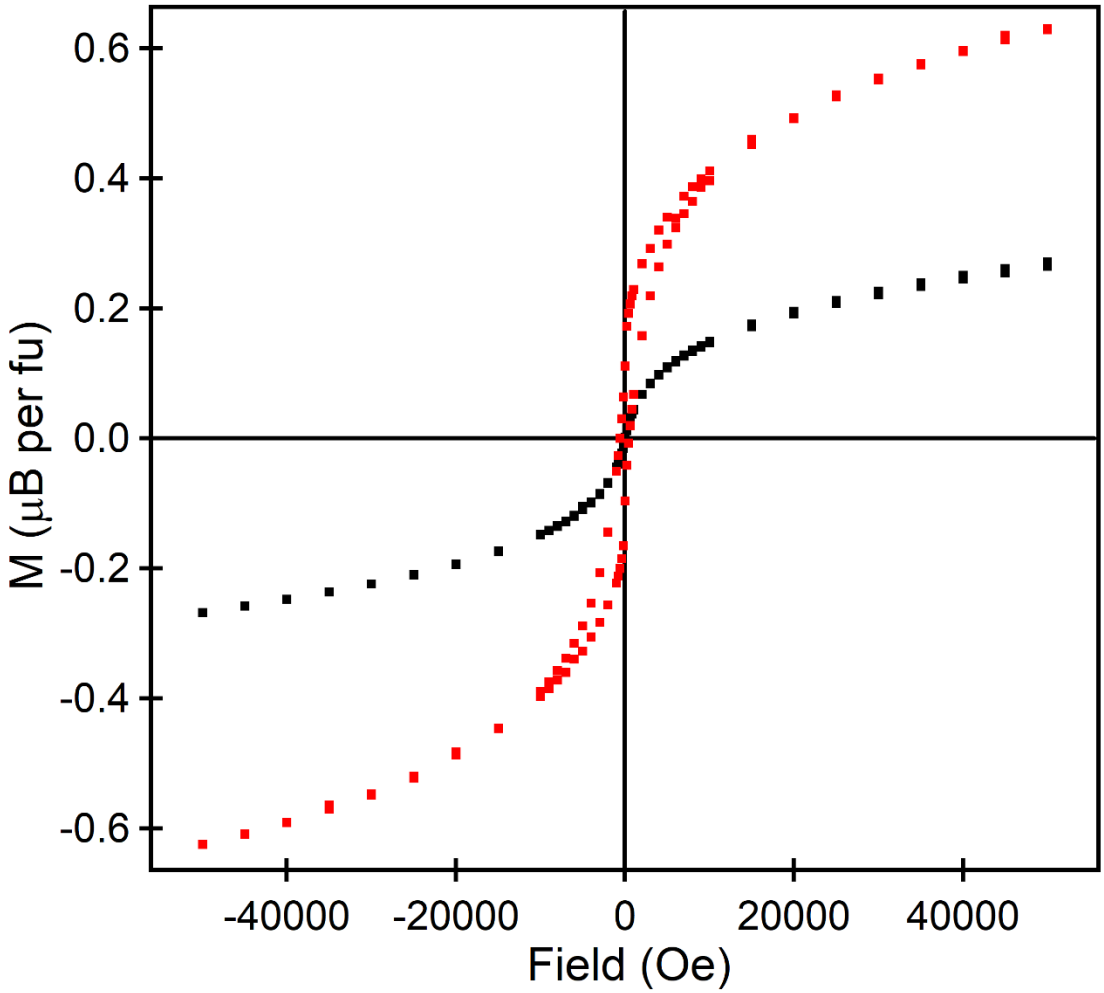


**Figure S18.** Magnetization-field data collected from $La_{0.5}Sr_{1.5}CoIrO_{2.5}H_{1.5}$ at 300 K and at 5 K after cooling from 300 K in an applied field of 5 T.

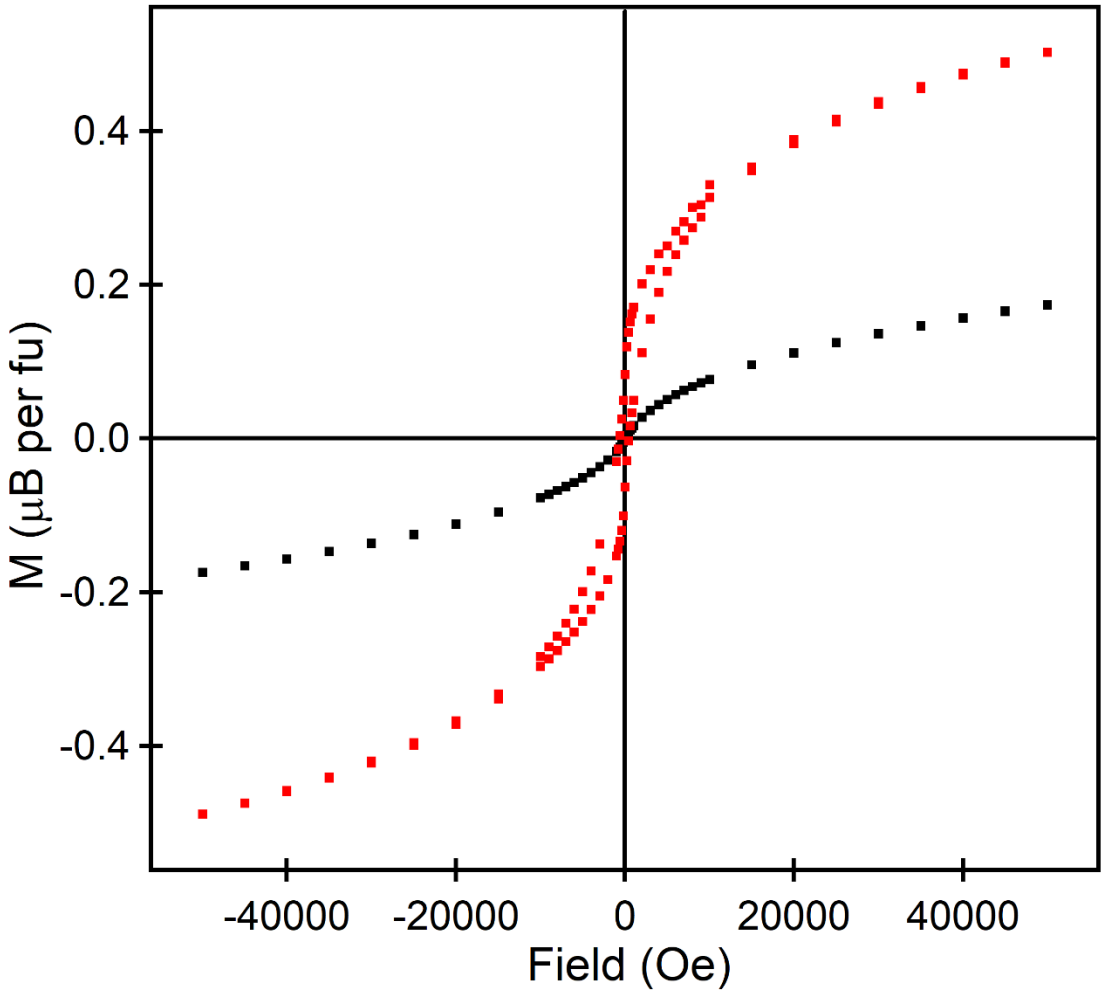


**Figure S19.** Magnetization-field data collected from $La_{0.75}Sr_{1.25}CoIrO_{2.75}H_{1.25}$ at 300 K and at 5 K after cooling from 300 K in an applied field of 5 T.

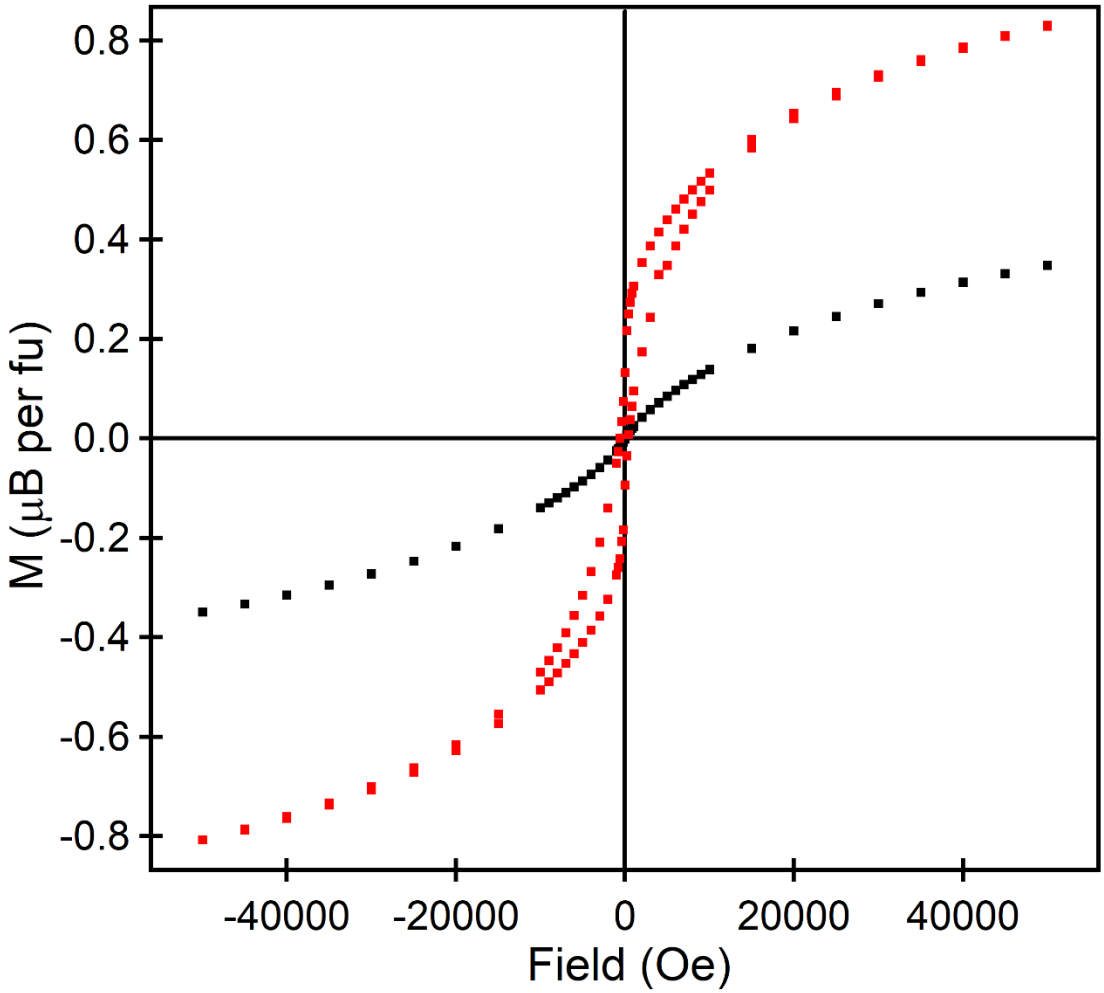


**Figure S20.** Magnetization-field data collected from $LaSrCo_{0.5}Ir_{0.5}O_3H$ at 300 K and at 5 K after cooling from 300 K in an applied field of 5 T.

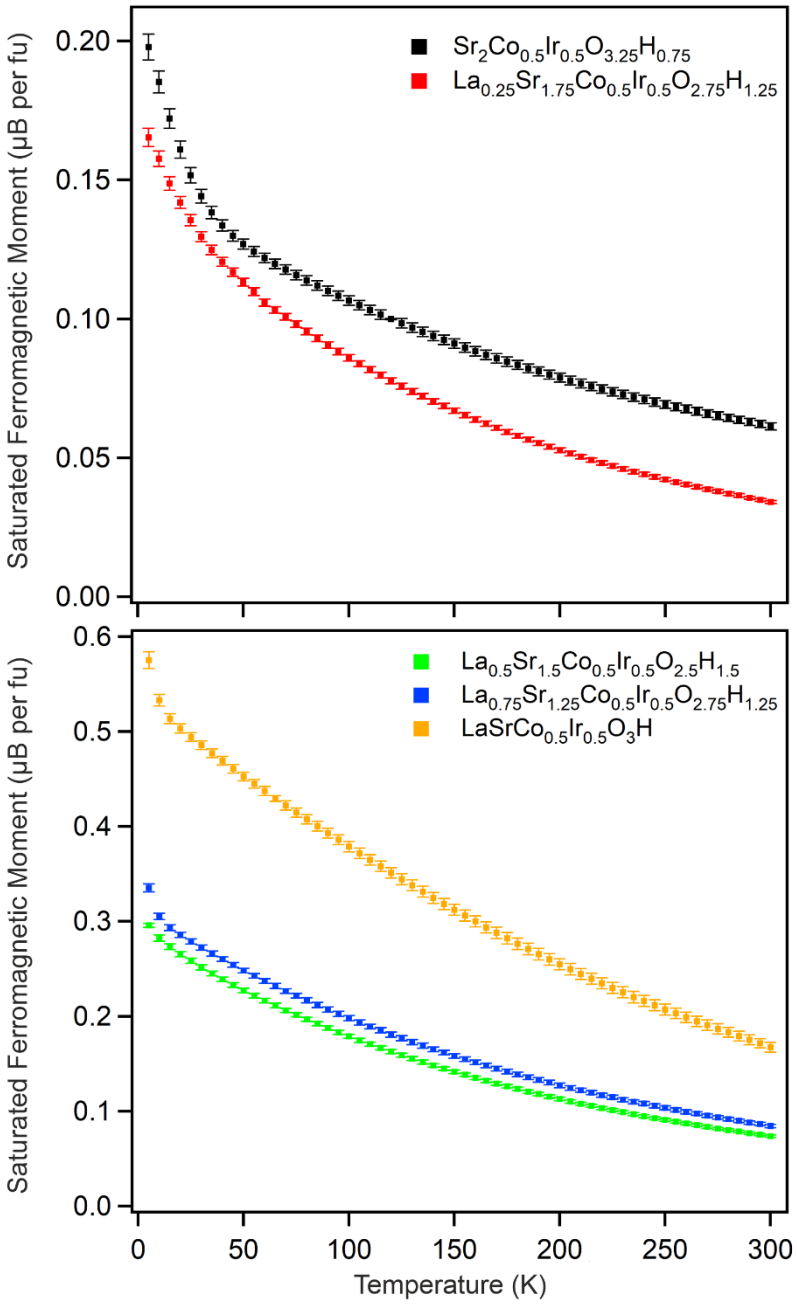


**Figure S21.** Saturated ferromagnetic moment obtained from 'ferrosubtraction' magnetization measurements plotted as a function of temperature for $La_xSr_{2-x}Co_{0.5}Ir_{0.5}O_{4-y}H_y$ phases.

## 5. Magnetic measurements in the presence of elemental Co impurities via the 'ferrosubtraction' method.

Procedure used to measure the magnetization of samples containing elemental cobalt:
The magnetization of elemental Co is observed to saturate in applied magnetic fields of more than 2 T. Thus, the paramagnetic susceptibility of a bulk sample can be measured in the presence of elemental Co impurities by measuring the gradient of magnetization-field isotherms in applied fields larger than 2 T. As shown in Figure S7.

To this end the magnetization of samples was measured in a series of 5 fields between 3 T and 5 T. The magnetization vs. field data were fitted to a linear function, the gradient of which is the paramagnetic susceptibility of the bulk sample and the intercept is the saturated ferromagnetic moment of the sample. Data points with large errors were excluded from fits. All fits had at least 4 data points. This procedure was repeated at 5 K intervals between 5 K and 300 K to measure the temperature dependent susceptibility of samples.

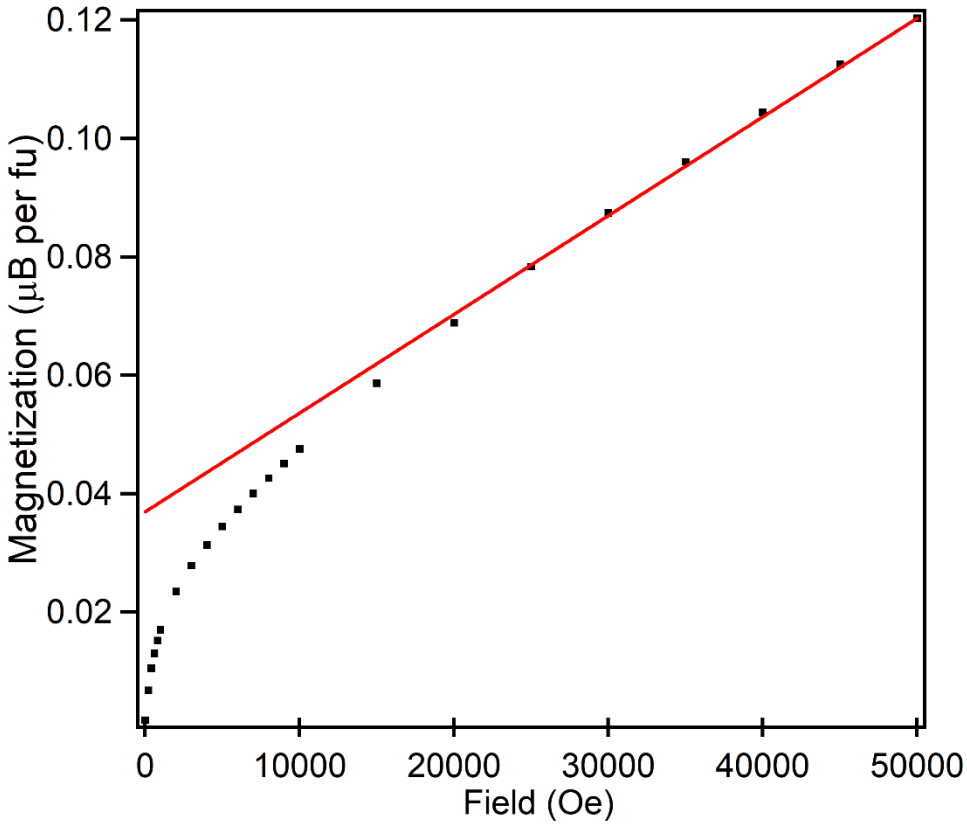


**Figure S22**. Magnetisation of $Sr_2Co_{0.5}Ir_{0.5}O_{3.25}H_{0.75}$ measured as a function of applied field at 300 K. A linear fit to high-field region (H > 25000 Oe) yields a gradient which is the paramagnetic susceptibility of the sample, and an intercept which is the saturated ferromagnetic moment of the sample.